

# 15.

## DYNAMIC ANALYSIS USING RESPONSE SPECTRUM SEISMIC LOADING

*Before the Existence of Inexpensive Personal Computers, the Response Spectrum Method was the Standard Approach for Linear Seismic Analysis*

### 15.1 INTRODUCTION

The first version of this chapter on the Response Spectrum Method was written over twenty five years ago with the purpose of improving the accuracy of this ***approximate linear method*** for the seismic loading and to provide guidelines for its practical uses. At that time, the author believed the method would be used for only a few more years and would soon be replaced by the more accurate, flexible and simple time-history seismic response analysis method for both ***linear and nonlinear analysis*** of complex structures. The recent increase in the speed and capacity of personal computers has made it practical to run many time-history analyses in a short period of time. The Current Speed of a \$1,000 Personal Computer is 56,000 times faster than the \$1,000,000 Computer of 1963 (See Appendix H). Also, in 1963 only a few recorded time-history earthquake records existed. At the present time, we have thousands of earthquake records available. Therefore, it is no longer necessary to use this very approximate and inaccurate spectrum methods of analysis.

Unfortunately, the use of more accurate analysis methods has not occurred. In fact, the use of the response spectrum method and other simplified static methods appears to have increased and the use of the more accurate time-history analysis methods has been reduced during the past several years. Also, many structural engineers believe an “Equivalent Static Analysis” like a pushover analysis is more accurate than a rigorous nonlinear analysis in which dynamic equilibrium is satisfied at each time step. Also, many structural engineers continue to claim they can solve nonlinear problems by “creating” nonlinear spectra. It appears they have forgotten that earthquake displacements are applied at the base of the structure and are then propagated upward into the structure to cause the lateral displacements in the superstructure.

Finally, an example will be given where a long bridge structure is retrofitted to resist realistic ground displacements that are different at each foundation. The retrofitted structure was designed

to behave nonlinearly to dissipate energy at a finite number of elements that would be easily repairable or replaced after a major earthquake.

## 15.2 DEFINITION OF A RESPONSE SPECTRUM

For three-dimensional seismic motion, the typical modal Equation (13.6) is rewritten as:

$$\ddot{y}(t)_n + 2\zeta_n \omega_n \dot{y}(t)_n + \omega_n^2 y(t)_n = p_{nx} \ddot{x}(t)_{gx} + p_{ny} \ddot{x}(t)_{gy} + p_{nz} \ddot{x}(t)_{gz} \quad (15.1)$$

Where, the three *Mode Participation Factors* are defined by  $p_{ni} = -\phi_n^T \mathbf{M}_i$  in which  $i$  is equal to  $x$ ,  $y$  or  $z$ . Two major problems must be solved to obtain an approximate response spectrum solution to this equation. First, for each direction of ground motion, maximum peak forces and displacements must be estimated. Second, after the response for the three orthogonal directions has been solved, it is necessary to estimate the maximum response from the three components of earthquake motion acting at the same time. This section addresses the modal combination problem from one component of motion only. The separate problem of combining the results from motion in three orthogonal directions will be discussed later in this chapter.

For input in one direction only, Equation (15.1) is written as:

$$\ddot{y}(t)_n + 2\zeta_n \omega_n \dot{y}(t)_n + \omega_n^2 y(t)_n = p_{ni} \ddot{x}(t)_g \quad (15.2)$$

Given a specified ground motion  $\ddot{x}(t)_g$ , damping value and assuming  $p_{ni} = -1.0$ , it is possible to solve Equation (15.2) at various values of  $\omega$  and plot a curve of the maximum peak response. For this acceleration input, the curve is by definition the **displacement response spectrum** for the earthquake motion. A different curve will exist for each different value of damping.

Structural engineers that use a response spectrum curve must understand the time the maximum peak value  $y(\omega)_{MAX}$  occurs has been lost in the creation of the curve and can be significantly different for each value of  $\omega$ . Therefore, combining responses from different modes will always be approximate. And, the internal member forces calculated are not in static equilibrium.

A plot of  $\omega y(\omega)_{MAX}$  is defined as the **pseudo-velocity spectrum** and a plot of  $\omega^2 y(\omega)_{MAX}$  is defined as the **pseudo-acceleration spectrum**.

The three curves—displacement response spectrum, pseudo-velocity spectrum, and pseudo-acceleration spectrum—are normally plotted as one curve on special log paper. However, the pseudo-values have minimum physical significance and are not an essential part of a response spectrum analysis. The true values for maximum velocity and acceleration must be calculated from the solution of Equation (15.2).

There is a mathematical relationship, however, between the pseudo-acceleration spectrum and the total acceleration spectrum. The total acceleration of the unit mass, single degree-of-freedom system, governed by Equation (15.2), is given by:

$$\ddot{x}(t)_T = \ddot{x}(t) + \ddot{x}(t)_g \quad (15.3)$$

Equation (15.2) can be solved for  $\ddot{x}(t)$  and substituted into Equation (15.3) to yield:

$$\ddot{x}(t)_T = -\omega^2 y(t) - 2\xi\omega\dot{y}(t) \quad (15.4)$$

Therefore, for the special case of zero damping, the total acceleration of the system is equal to  $\omega^2 y(t)$ . For this reason, the **displacement response spectrum** curve is normally not plotted as modal displacement  $y(\omega)_{MAX}$  versus  $\omega$ . It is standard to present the curve in terms of  $S(\omega)$  versus a period  $T$  in seconds, where:

$$S(\omega)_a = \omega^2 y(\omega)_{MAX} \quad \text{and} \quad T = \frac{2\pi}{\omega} \quad (15.5a \text{ and } 15.5b)$$

The pseudo-acceleration spectrum curve,  $S(\omega)_a$ , has the units of acceleration versus period that has some physical significance for zero damping only. It is apparent that all response spectrum curves represent the properties of the earthquake at a specific site and are not a function of the properties of the structural system. After an estimation is made of the linear viscous damping properties of the structure, a specific response spectrum curve is selected.

### 15.3 CALCULATION OF MODAL RESPONSE

The maximum modal displacement for a structural model can now be calculated for a typical mode  $n$  with period  $T_n$  and corresponding spectrum response value  $S(\omega_n)$ . The maximum modal response associated with period  $T_n$  is given by:

$$y(T_n)_{MAX} = \frac{S(\omega_n)}{\omega_n^2} \quad (15.6)$$

The maximum modal displacement response of the structural model is calculated from:

$$\mathbf{u}_n = y(T_n)_{MAX} \phi_n \quad (15.7)$$

The corresponding internal modal forces,  $f_{kn}$ , are calculated from standard matrix structural analysis using the same equations as required in static analysis.

### 15.4 CREATION OF RESPONSE SPECTRUM CURVES

A ten-second segment of the Loma Prieta earthquake motions recorded on a soft site in the San Francisco Bay Area is shown in Figure 15.1a. The record has been corrected using an iterative algorithm for zero displacement, velocity and acceleration at the beginning and end of the ten-second record.

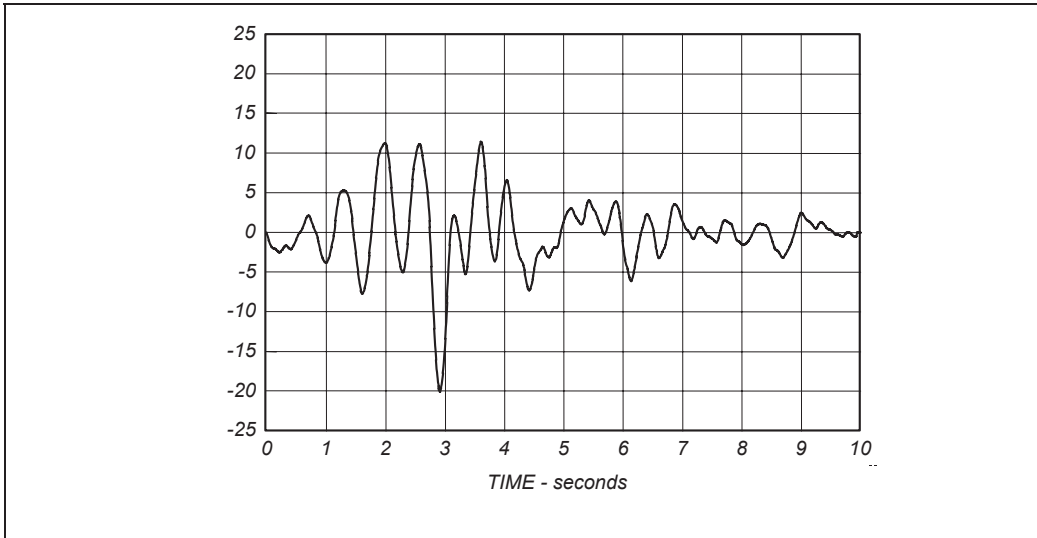


**Figure 15.1a Typical Earthquake Ground Acceleration - Percent of Gravity**

From the recorded earthquake accelerations shown in Figure 15.1a, the resulting ground displacements are calculated by numerical integrating the record twice and the plot of the results ground displacements is shown in Figure 15.1b.

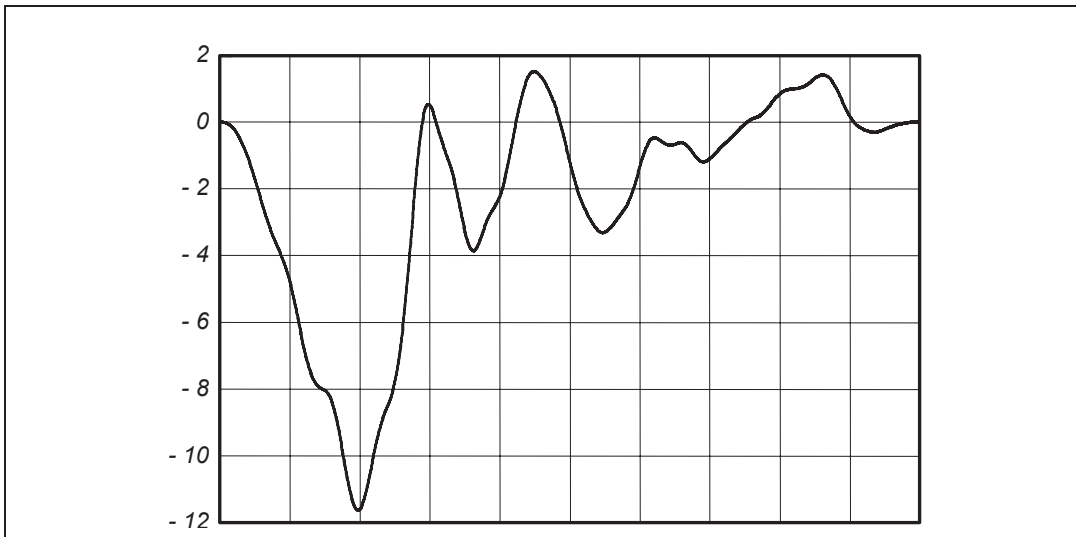


**Figure 15.1b Typical Earthquake Ground Displacements - Inches**

The

response spectrum curves for the relative displacement with respect zero ground displacement and pseudo-acceleration are calculated from Equations 15.2 and 15.6 are summarized below in Figure 15.2a and 15.2b.

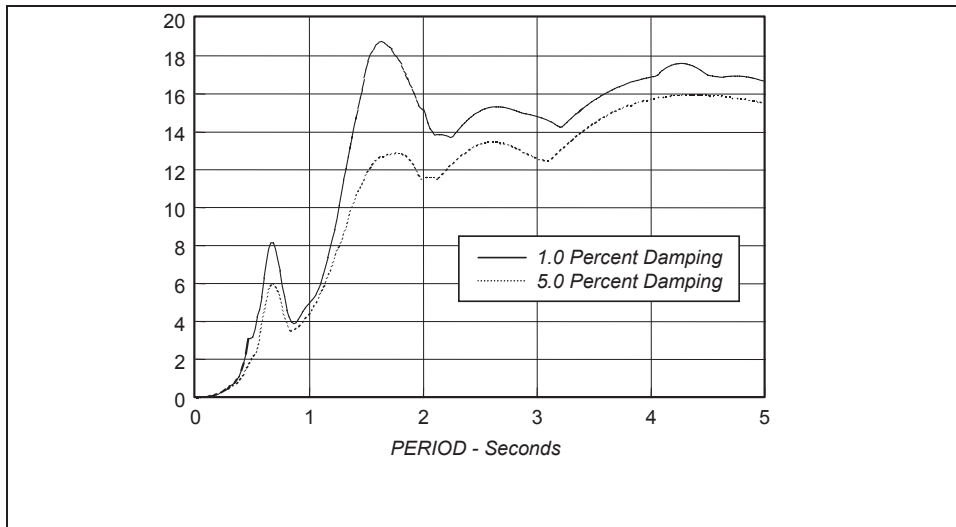


**Figure 15.2a Relative Displacement Spectrum  $y(\omega)_{MAX}$  - Inches**

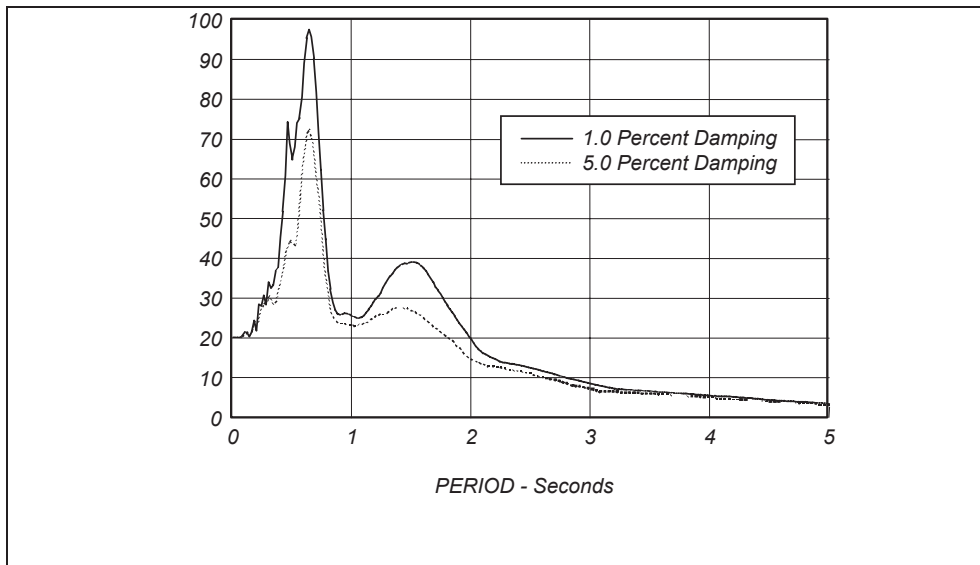


**Figure 15.2b Pseudo-Acceleration Spectrum,  $S_a = \omega^2 y(\omega)_{MAX}$  Percent of Gravity**

The maximum ground acceleration for the earthquake defined by Figure 15.1a is 20.01 percent of gravity at 2.92 seconds. It is important to note that the pseudo-acceleration spectrum shown in Figure 15.2b has the same value for a very short period system. This is because of the physical fact that a very rigid structure moves as a rigid body and the relative displacements within the structure are equal to zero, as indicated by Figure 15.2a. Also, the behavior of a rigid structure is not a function of the viscous damping value.

The maximum ground displacement shown in Figure 15.1b is -11.62 inches at 1.97 seconds. For long period systems, the mass of the one-degree-of-freedom structure does not move significantly

and has approximately zero absolute displacement. Therefore, the relative displacement spectrum curves shown in Figure 15.2a will converge to 11.62 inches for long periods and all values of damping. This type of real physical behavior is fundamental to the design of base isolated structures.

The relative displacement spectrum, Figure 15.2a, and the absolute acceleration spectrum, Figure 15.2b, have physical significance. However, the maximum relative displacement is directly proportional to the maximum forces developed in the structure. For that earthquake, the maximum relative displacement is 18.9 inches at a period of 1.6 seconds for 1 percent damping and 16.0 inches at a period of 4 seconds for 5 percent damping. It is important to note the significant difference between 1 and 5 percent damping for this typical soft site record.

Figure 15.2b, the absolute acceleration spectrum, indicates maximum values at a period of 0.64 seconds for both values of damping. Also, the multiplication by  $\omega^2$  tends to completely eliminate the information contained in the long period range. Because most structural failures during recent earthquakes have been associated with soft sites, perhaps we should consider using the relative displacement spectrum as the fundamental form for selecting a design earthquake. The high-frequency, short-period part of the curve should always be defined by:

$$y(\omega)_{MAX} = \ddot{x}_{gMAX} / \omega^2 \quad \text{or} \quad y(T)_{MAX} = \ddot{x}_{gMAX} \frac{T^2}{4\pi^2} \quad (15.8)$$

where  $\ddot{x}_{gMAX}$  is the peak ground acceleration.

## 15.5 THE SRSS and CQC METHOD OF MODAL COMBINATION

The most conservative method that is used to estimate a peak value of displacement or force within a structure is to use the sum of the absolute of the modal response values. This approach assumes that the maximum modal values for all modes occur at the same point in time.

Another very common approach is to use the Square Root of the Sum of the Squares, SRSS, on the maximum modal values to estimate the values of displacement or forces. The SRSS method assumes that all of the maximum modal values are statistically independent. For three-dimensional structures in which a large number of frequencies are almost identical, this assumption is not justified. However, it was used until the mid eighties.

The modal combination by the Complete Quadratic Combination, CQC, method [1] that was first published in 1981. It is based on random vibration theories and has found wide acceptance by most engineers and has been incorporated as an option in most modern computer programs for seismic analysis. Because many engineers and building codes are not requiring the use of the CQC method, one purpose of this chapter is to explain by example the advantages of using the CQC method and illustrate the potential problems in the use of the SRSS method of modal combination.

The peak value of a typical force can now be estimated from the maximum modal values using the CQC method with the application of the following double summation equation:

$$F = \sqrt{\sum_n \sum_m f_n \rho_{nm} f_m} \tag{15.9}$$

where  $f_n$  is the modal force associated with mode  $n$ . The double summation is conducted over all modes. Similar equations can be applied to node displacements, relative displacements and base shears and overturning moments.

The cross-modal coefficients,  $\rho_{nm}$ , for the CQC method with constant damping are:

$$\rho_{nm} = \frac{8\zeta^2(1+r)r^{3/2}}{(1-r^2)^2 + 4\zeta^2r(1+r)^2} \tag{15.10}$$

where  $r = \omega_n / \omega_m$  and must be equal to or less than 1.0. It is important to note that the cross-modal coefficient array is symmetric and all terms are positive.

### 15.6 NUMERICAL EXAMPLE OF MODAL COMBINATION

The problems associated with using the absolute sum and the SRSS of modal combination can be illustrated by their application to the four-story building shown in Figure 15.3. The building is symmetrical; however, the center of mass of all floors is located 25 inches from the geometric center of the building.

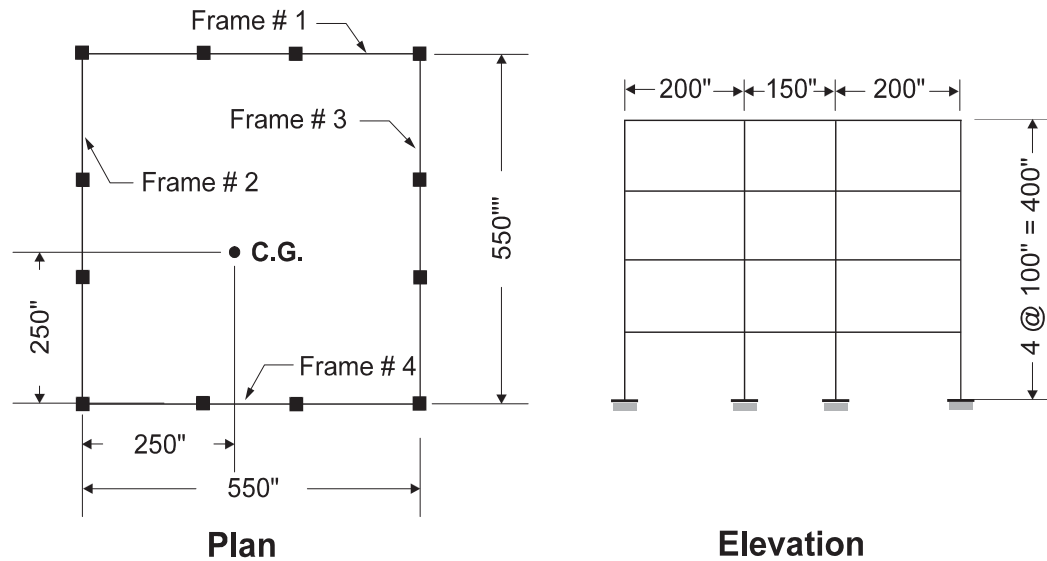


*Figure 15.3 A Simple Three-Dimensional Building Example*

The direction of the applied earthquake motion, a table of natural frequencies and the principal direction of the mode shape are summarized in Figure 15.4.

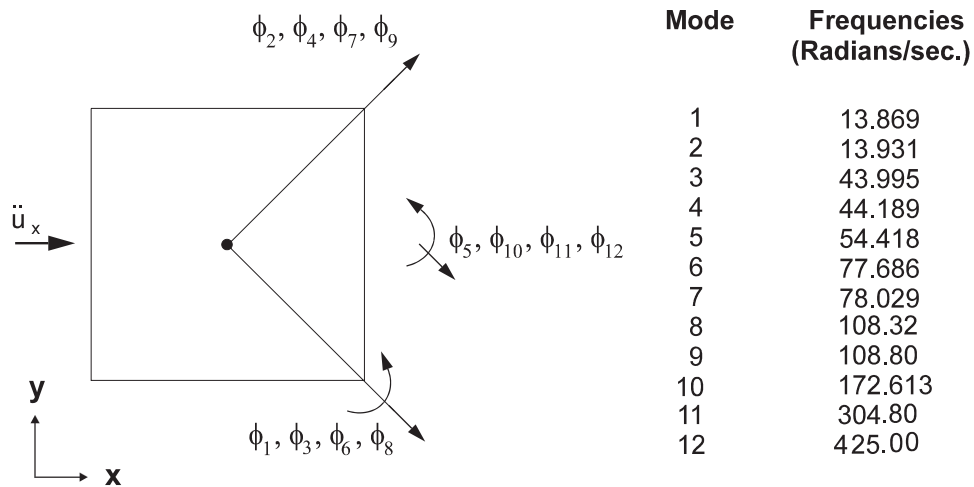


**Figure 15.4** Frequencies and Approximate Directions of Mode Shapes

One notes the closeness of the frequencies that is typical of most three-dimensional building structures that are designed to resist earthquakes from both directions equally. Because of the small mass eccentricity, which is normal in real structures, the fundamental mode shape has  $x$ ,  $y$ , as well as torsion components. Therefore, the model represents a very common three-dimensional building system. Also, note that there *is not a mode shape in a particular given direction*, as is implied in many building codes and some text books on elementary dynamics.

The building was subjected to one component of the Taft 1952 earthquake. An exact time history analysis using all 12 modes and a response spectrum analysis were conducted. The maximum modal base shears in the four frames for the first five modes are shown in Figure 15.5.

Figure 15.6 summarizes the maximum base shears in each of the four frames using different methods. The time history base shears, Figure 15.6a, are exact. The SRSS method, Figure 15.6b, produces base shears that under-estimate the exact values in the direction of the loads by approximately 30 percent and over-estimate the base shears normal to the loads by a factor of 10. The sum of the absolute values, Figure 15.6c, grossly over-estimates all results. The CQC method, Figure 15.6d, produces very realistic values that are close to the exact time history solution.



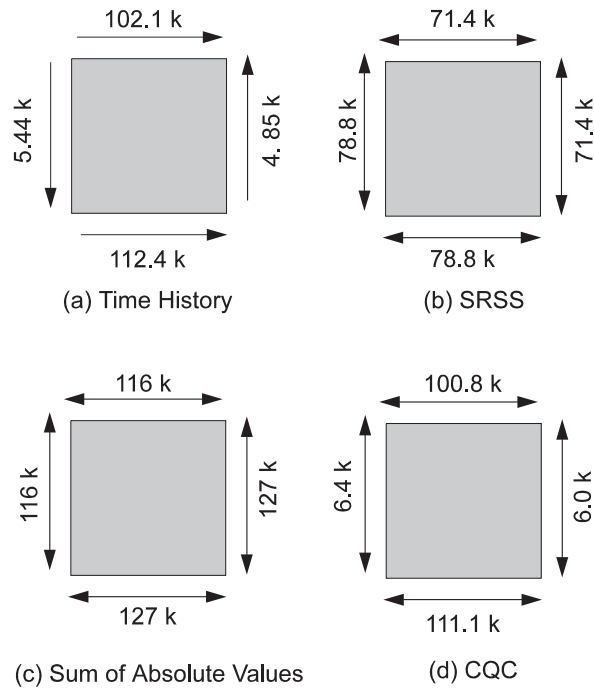
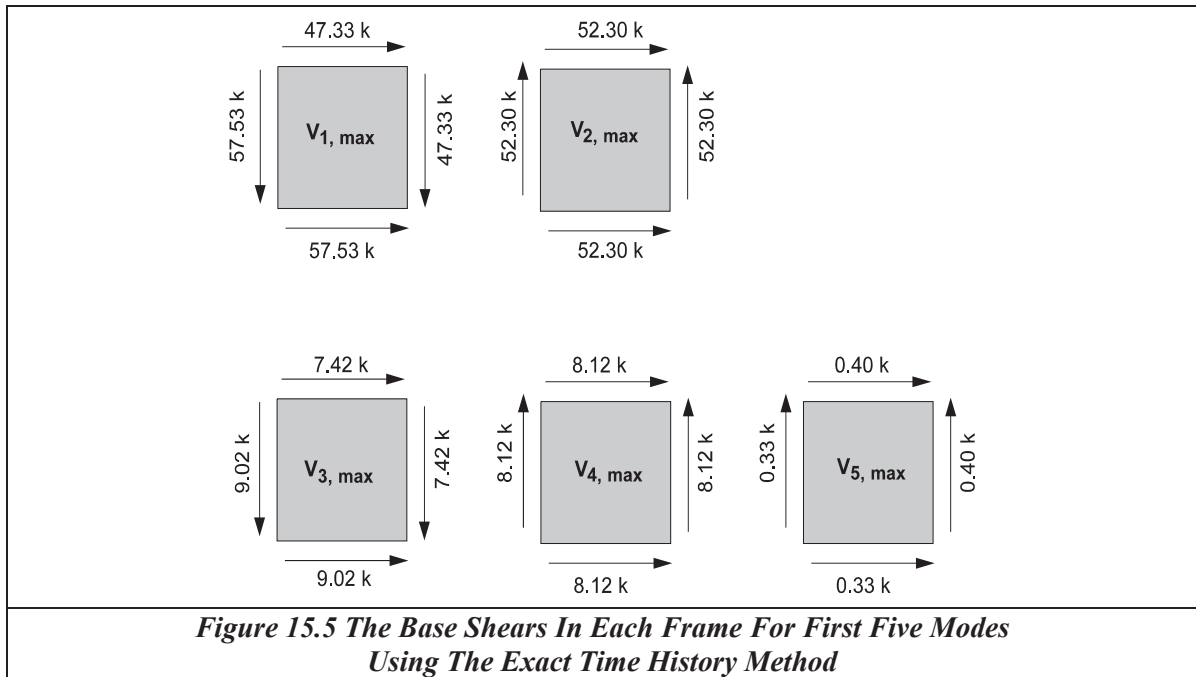


**Figure 15.6 Comparison of Modal Combination Methods**

The modal cross-correlation coefficients for this building are summarized in Table 15.1. It is of importance to note the existence of the relatively large off-diagonal terms that indicate which modes are coupled.

**Table 15.1 Modal Cross-Correlation Coefficients -  $\zeta = 0.05$** 

Mode	1	2	3	4	5	$\omega_n$ (rad/sec)
1	1.000	0.998	0.006	0.006	0.004	13.87
2	0.998	1.000	0.006	0.006	0.004	13.93
3	0.006	0.006	1.000	0.998	0.180	43.99
4	0.006	0.006	0.998	1.000	0.186	44.19
5	0.004	0.004	0.180	0.186	1.000	54.42

If one notes the signs of the modal base shears shown in Figure 15.3, it is apparent how the application of the CQC method allows the sum of the base shears in the direction of the external motion to be added directly. In addition, the sum of the base shears, normal to the external motion, tend to cancel. The ability of the CQC method to recognize the relative sign of the terms in the modal response is the key to the elimination of errors in the SRSS method.

## 15.7 DESIGN SPECTRA

Design spectra are not uneven curves as shown in Figure 15.2 because they are intended to be the average of many earthquakes. At the present time, many building codes specify design spectra in the form shown in Figure 15.7.

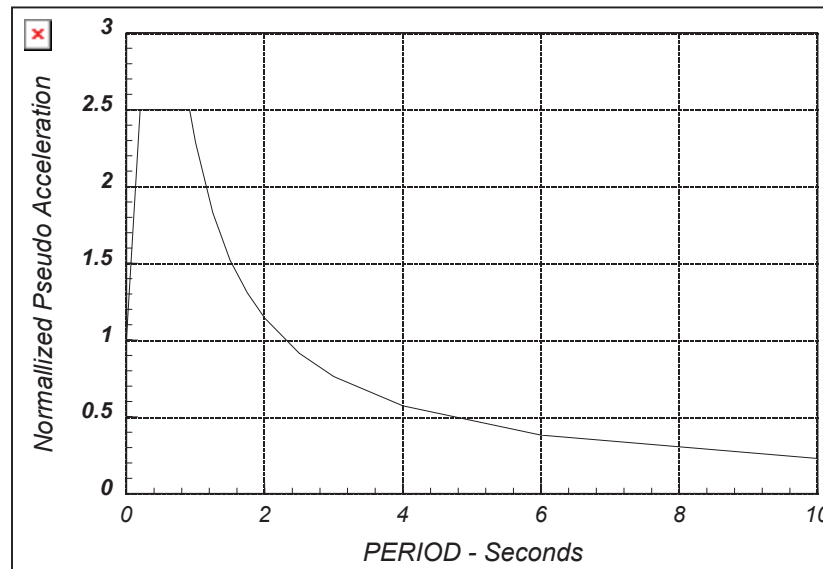


**Figure 15.7 Typical Design Spectrum**

The Uniform Building Code has defined specific equations for each range of the spectrum curve for four different soil types. For major structures, it is now common practice to develop a site-dependent design spectrum that includes the effect of local soil conditions and distance to the nearest faults.

## 15.8 ORTHOGONAL EFFECTS IN SPECTRAL ANALYSIS

A well-designed structure should be capable of equally resisting earthquake motions from all possible directions. One option in existing design codes for buildings and bridges requires that members be designed for "100 percent of the prescribed seismic forces in one direction plus 30 percent of the prescribed forces in the perpendicular direction." However, they give no indication on how the directions are to be determined for complex structures. For structures that are rectangular and have clearly defined principal directions, these "percentage" rules yield approximately the same results as the SRSS method.

For complex three-dimensional structures, such as non-rectangular buildings, curved bridges, arch dams or piping systems, the direction of the earthquake that produces the maximum stresses in a particular member or at a specified point is not apparent. For time history input, it is possible to perform a large number of dynamic analyses at various angles of input to check all points for the critical earthquake directions. Such an elaborate study could conceivably produce a different critical input direction for each stress evaluated. However, the cost of such a study would be prohibitive.

It is reasonable to assume that motions that take place during an earthquake have one principal direction [2]. Or, during a finite period of time when maximum ground acceleration occurs, a principal direction exists. For most structures, this direction is not known and for most geographical locations cannot be estimated. Therefore, the only rational earthquake design criterion is that the structure must resist an earthquake of a given magnitude from any possible direction. In addition to the motion in the principal direction, a probability exists that motions normal to that direction will occur simultaneously. In addition, because of the complex nature of three-dimensional wave propagation, it is valid to assume that these normal motions are statistically independent.

Based on those assumptions, a statement of the design criterion is "a structure must resist a major earthquake motion of magnitude  $S_1$  for all possible angles  $\theta$  and at the same point in time resist earthquake motions of magnitude  $S_2$  at  $90^\circ$  to the angle  $\theta$ ." These motions are shown schematically in Figure 15.1.

### 15.8.1 Basic Equations for Calculation of Spectral Forces

The stated design criterion implies that a large number of different analyses must be conducted to determine the maximum design forces and stresses. It will be shown in this section that maximum values for all members can be exactly evaluated from one computer run in which two global dynamic motions are applied. Furthermore, the maximum member forces calculated are invariant with respect to the selection system.

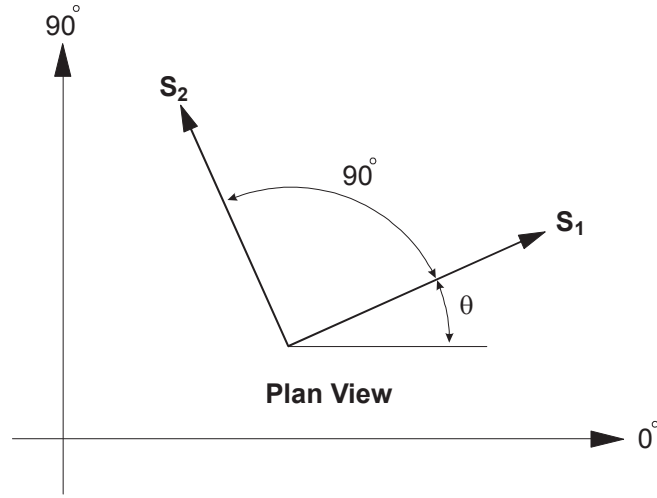


**Figure 15.8 Definition of Earthquake Spectra Input**

Figure 15.8 indicates that the basic input spectra  $S_1$  and  $S_2$  are applied at an arbitrary angle  $\theta$ . At some typical point within the structure, a force, stress or displacement  $F$  is produced by this input. To simplify the analysis, it will be assumed that the minor input spectrum is some fraction of the major input spectrum. Or:

$$S_2 = aS_1 \quad (15.11)$$

where  $a$  is a number between 0 and 1.0.

Recently, Menun and Der Kiureghian [3] presented the CQC3 method for the combination of the effects of orthogonal spectrum.

The fundamental CQC3 equation for the estimation of a peak value is:

$$F = [F_0^2 + a^2 F_{90}^2 - (1 - a^2)(F_0^2 - F_{90}^2) \sin^2 \theta + 2(1 - a^2)F_{0-90} \sin \theta \cos \theta + F_z^2]^{\frac{1}{2}} \quad (15.12)$$

where,

$$F_0^2 = \sum_n \sum_m f_{0n} \rho_{nm} f_{0m} \quad (15.13)$$

$$F_{90}^2 = \sum_n \sum_m f_{90n} \rho_{nm} f_{90m} \quad (15.14)$$

$$F_{0-90} = \sum_n \sum_m f_{0n} \rho_{nm} f_{90m} \quad (15.15)$$

$$F_z^2 = \sum_n \sum_m f_{zn} \rho_{nm} f_{zm} \quad (15.16)$$

in which  $f_{0n}$  and  $f_{90n}$  are the modal values produced by 100 percent of the lateral spectrum applied at 0 and 90 degrees respectively, and  $f_{zn}$  is the modal response from the vertical spectrum that can be different from the lateral spectrum.

It is important to note that for equal spectra  $a=1$ , the value  $F$  is not a function of  $\theta$  and the selection of the analysis reference system is arbitrary. Or:

$$F_{MAX} = \sqrt{F_0^2 + F_{90}^2 + F_z^2} \quad (15.17)$$

This indicates that it is possible to conduct only one analysis with any reference system, and the resulting structure will have all members that are designed to equally resist earthquake motions from all possible directions. This method is acceptable by most building codes.

### 15.8.2 The General CQC3 Method of modal combination

For  $a=1$ , the CQC3 method reduces to the SRSS method. However, this can be over conservative because real ground motions of equal value in all directions have not been recorded. Normally, the value of  $\theta$  in Equation (15.12) is not known; therefore, it is necessary to calculate the critical angle that produces the maximum response. Differentiation of Equation (15.12) and setting the results to zero yields:

$$\theta_{cr} = \frac{1}{2} \tan^{-1} \left[ \frac{2F_{0-90}}{F_0^2 - F_{90}^2} \right] \quad (15.18)$$

Two roots exist for Equation (15.17) that must be checked in order that the following equation is maximum:

$$F_{MAX} = [F_0^2 + a^2 F_{90}^2 - (1 - a^2)(F_0^2 - F_{90}^2) \sin^2 \theta_{cr} - 2(1 - a^2)F_{0-90} \sin \theta_{cr} \cos \theta_{cr} + F_z^2]^{\frac{1}{2}} \quad (15.19)$$

At the present time, no specific guidelines have been suggested for the value of  $a$ . Reference [3] presented an example with values  $a$  between 0.50 and 0.85.

### 15.8.3 Examples of Three-Dimensional Spectra Analyses

The previously presented theory clearly indicates that the CQC combination rule, with  $a$  equal to 1.0, is identical to the SRSS method and produces results for all structural systems that are not a function of the reference system used by the engineer. One example will be presented to show the advantages of the method. Figure 15.9 illustrates a very simple one-story structure that was selected to compare the results of the 100/30 percentage rules with the SRSS rule.

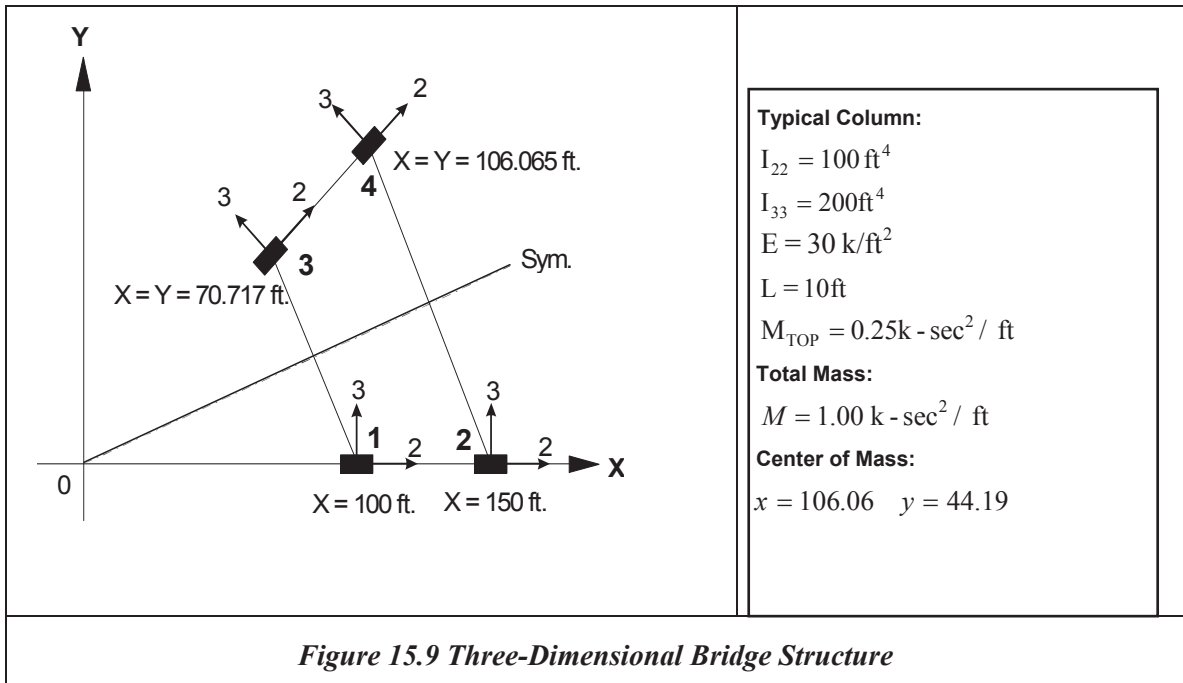


Figure 15.9 Three-Dimensional Bridge Structure

Note that the masses are not at the geometric center of the structure. The structure has two translations and one rotational degrees-of-freedom located at the center of mass. The columns, which are subjected to bending about the local 2 and 3 axes, are pinned at the top where they are connected to an in-plane rigid diaphragm.

The periods and normalized base shear forces associated with the mode shapes are summarized in Table 15.2. Because the structure has a plane of symmetry at 22.5 degrees, the second mode has no torsion and has a normalized base shear at 22.5 degrees with the x-axis. Because of this symmetry, it is apparent that columns 1 and 3 (or columns 2 and 4) should be designed for the same forces.

Table 15.2 Periods and Normalized Base Shear

Mode	Period (Seconds)	X-Force	Y-Force	Direction of Base Shear (Degrees)
1	1.047	0.383	-0.924	-67.5
2	0.777	-0.382	0.924	112.5 <i>Torsion</i>
3	0.769	0.924	0.383	22.5

The displacement response spectrum used in the spectra analysis is given in Table 15.3.

**Table 15.3 Participating Masses and Response Spectrum Used**

Mode	Period (Seconds)	X-Mass	Y-Mass	Spectral Value Used for Analysis
1	1.047	12.02	70.05	1.00
2	0.777	2.62	15.31	1.00
3	0.769	85.36	14.64	1.00

The moments about the local 2 and 3 axes at the base of each of the four columns for the spectrum applied separately at 0.0 and 90 degrees are summarized in Tables 15.4 and 15.5 and are compared to the 100/30 rule.

**Table 15.4 Moments About 2-Axes – SRSS vs. 100/30 Rule**

Member	$M_0$	$M_{90}$	$M_{SRSS} = \sqrt{M_0^2 + M_{90}^2}$	$M_{100/30}$	Error(%)
1	0.742	1.750	1.901	1.973	3.8
2	1.113	2.463	2.703	2.797	3.5
3	0.940	1.652	1.901	1.934	1.8
4	1.131	2.455	2.703	2.794	3.4

**Table 15.5 Moments About 3-Axes – SRSS vs. 100/30 Rule**

Member	$M_0$	$M_{90}$	$M_{SRSS} = \sqrt{M_0^2 + M_{90}^2}$	$M_{100/30}$	Error(%)
1	2.702	0.137	2.705	2.743	1.4
2	2.702	0.137	2.705	2.743	1.4
3	1.904	1.922	2.705	2.493	-7.8
4	1.904	1.922	2.705	2.493	-7.8

For this example, the maximum forces do not vary significantly between the two methods. However, it does illustrate that the 100/30 combination method produces moments that are not symmetric, whereas the SRSS combination method produces logical and symmetric moments. For example, member 4 would be over-designed by 3.4 percent about the local 2-axis and under-designed by 7.8 percent about the local 3-axis using the 100/30 combination rule.

## 15.9 Demand/Capacity Calculations for 3D Frame Elements

In order to satisfy various building codes specify that all one-dimensional **compression** members within a structure satisfies the following Demand/Capacity Ratio at all points in time:

$$R(t) = \frac{|P(t)|}{\phi_c P_{cr}} \pm \frac{M_2(t) C_2}{\phi_b M_{c2} \left(1 - \frac{|P(t)|}{P_{e2}}\right)} \pm \frac{M_3(t) C_3}{\phi_b M_{c3} \left(1 - \frac{|P(t)|}{P_{e3}}\right)} \leq 1.0 \quad (15.20)$$

Where the forces acting on the frame element cross-section at time “t” are  $P(t)$ ,  $M_2(t)$  and  $M_3(t)$  (including the static forces prior to the application of the dynamic loads). The empirical constants are code and material dependent and are normally defined as

$\phi_c$ and $\phi_b$	=	Resistance factors
$C_2$ and $C_3$	=	Moment reduction factors
$M_{c2}$ and $M_{c3}$	=	Moment capacity
$P_{cr}$	=	Axial load Capacity
$P_{e2}$ and $P_{e3}$	=	Euler bucking load capacity about the 2 and 3 axis with effective length approximated.

For each **time-history seismic analysis**,  $P(t)$ ,  $M_2(t)$  and  $M_3(t)$  at every cross-section of all members can be easily calculated as a function of time. Therefore, the maximum Demand/Capacity Ratio,  $R(t)$  for all load conditions, can be accurately calculated and identified by any modern computer analysis design program in a fraction of a second. All of the CSI series of programs have this capability built into their interactive post-processing programs.

For each **response spectrum analysis**, however, the value of  $P(t)$ ,  $M_2(t)$  and  $M_3(t)$  cannot be calculated accurately since only positive values of  $P$ ,  $M_2$  and  $M_3$  are produced. These are peak maximum values have a very low probability of occurring at the same time. Therefore, the Demand/Capacity Ratios are always significantly greater than those produced by a time-history analysis.

The author, acting as a consultant on the retrofit of the San Mateo Bridge after the Loma Prieta Earthquake, has had significant experience with the problem of calculating Demand/Capacity Ratios using the response spectra method. The seismologists and geotechnical engineers created two different sets of three-dimensional ground motions. They generated both near and far field motions from both the Hayward and San Andreas faults. Then, they averaged the various ground motions and produced three-dimensional design spectra to be used to design the retrofit of the Bridge.



The structural engineering group that tried to use the design spectra for the analysis and retrofit of the bridge found that a large number of members in the structure required retrofit. After a careful study of the maximum peak values of the member forces (especially the large peak axial forces), it was decided to run new time-history analyses using the basic time-history records that were used to create the design spectra. After running all the time-history records, the maximum *Demand/Capacity Ratios were reduced by approximately a factor of three compared to the design spectra results.*

SAP90 was used for this project in approximately 1997 prior to the release of SAP2000. The major amount of manpower was in creating the computer model of the structure for the response spectra analyses. The time-history post-processing calculations of the maximum Demand/Capacity Ratios were calculated for all members in a series of simple overnight computer runs. Therefore, there was not a significant increase in manpower or time to obtain very accurate results (which satisfied dynamic force equilibrium) as compared to the very poor results obtained from use of spectra input.

### 15.10 Example of a very Complex Seismic Retrofit Project

After the completion of the retrofit design for the San Mateo Bridge the same structural engineering group started working on the retrofit design of the Richmond-San Rafael Bridge. This bridge was a very complex double-deck steel truss structure built in the mid nineteen fifties. Also, significant nonlinear behavior was expected in the retrofitted structure since the purpose of the retrofit was to prevent collapse. In addition, the time-history seismic displacements were different at each pier foundation level. Clearly the response spectrum method could not possibly model the nonlinear behavior and the multi-support displacement input.

During the previous several years the author had developed a new method to accurately solve a certain class of nonlinear problems using the dynamic mode superposition method plus additional static modes associated with the nonlinear elements (see Fast Nonlinear Analysis - Chapter 18). This new method FNA was implemented in my personal research and development program, SADSAP, which had the same input data format as SAP90. This author wanted them to use this new method for the project in order to evaluate the FNA method on a large and significant project. They accepted my offer and I agreed to modify the program to meet their need and to provide free consulting services during the life of the project. Needless to say, I was very busy for the next few years attending meetings and making modifications to the SADSAP program. The retrofitted structure was designed to behave nonlinearly to dissipate energy at a finite number of elements that would be easily repairable or replaced after a major earthquake. The Demand/Capacity Ratios reflected the redistribution of forces due to nonlinear behavior as well as the opening and closing of all joints.

Within a year after the successful completion of the project, CSI released SAP2000, which is a Windows based program, added an improved version of the FNA method of nonlinear analysis and many other valuable options.

### 15.11 SUMMARY

In this chapter it has been illustrated that the response spectrum method of dynamic analysis is a very approximate method for structures over one degree of freedom. The CQC method of modal combination and the SRSS to combine the response from any two orthogonal directions is the theoretically correct approach to apply the approximate response spectrum method. Also, this very approximate method can never be extended to produce correct results for the nonlinear seismic analysis of real structures.

During the last twenty years numerical methods for both linear and nonlinear time-history dynamic analysis have improved significantly. CSI has increased the speed of all phases of structural analysis by effectively using the power of the new multiprocessor chips. The use of 64 bit addressing capabilities has increased the size and complexity of the structures it can now solve on inexpensive personal computers. Within the last few years their programs have been used for analysis and design of the largest structures ever built.

### 15.12 REFERENCES

1. Wilson, E. L., A. Der Kiureghian and E. R. Bayo. 1981. "A Replacement for the SRSS Method in Seismic Analysis," *Earthquake Engineering and Structural Dynamics*. Vol. 9. pp. 187-192.
2. Penzien, J., and M. Watabe. 1975. "Characteristics of 3-D Earthquake Ground Motions," *Earthquake Engineering and Structural Dynamics*. Vol. 3. pp. 365-373.
3. Menun, C., and A. Der Kiureghian. 1998. "A Replacement for the 30 % Rule for Multicomponent Excitation," *Earthquake Spectra*. Vol. 13, Number 1. February.